Anal. Methods Environ. Chem. J. 8 (3) (2025) 31-46

AMECJ

Research Article, Issue 3

Analytical Methods in Environmental Chemistry Journal

Journal home page: www.amecj.com/ir

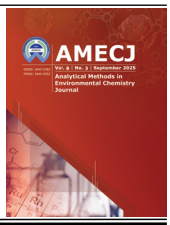

Evaluation and analysis of new complexes of luminol as a chemiluminescent material for biological samples by spectroscopy methods

Ban Khalil Ali[*,a]

[a]*Directorate of Thi Qar Education, Iraqi Ministry of Education, Thi Qar, Iraq*

ARTICLE INFO:

Received 30 Apr 2025

Revised form 9 Jul 2025

Accepted 16 Aug 2025

Available online 30 Sep 2025

Keywords:

Azo dyes, ligands,
Metal complex,
Luminol,
Spectrophotometry,
Bacteria

ABSTRACT

In this study, we present new metal complexes of Cr(II), Co(II), and Ni(II) synthesized using novel ligands produced through azo coupling between luminol and sulfamethoxazole. UV-Vis, FT-IR, ^{1}H NMR, and ^{13}C NMR spectroscopy were used to characterize the produced ligands and their complexes. UV-Vis results indicate that the maximum difference in absorbance wavelengths (λ max) was observed for the azo dye ligand and its respective metal complex, indicating successful coordination. Calibration curves constructed at the wavelengths specified for each complex are reported to exhibit excellent linearity within the range of 1.0-20.0 mg mL^{-1} (R^2> 0.998). The limits of detection LOD and quantification LOQ were determined to be 0.18 and 0.55 µg mL^{-1}, respectively. The method met the conditions for precision, as expressed by the relative standard deviation (RSD%), and was thus shown to have high reproducibility, with an RSD% below 2.5% (n = 5). Recovery studies were performed using known standards to spike analytes with recoveries ranging from 97.2% to 102.1%, indicating the method is accurate. The complexes were stable under varying pH, temperature, and time conditions. Job's and molar ratio methods confirmed 1:2 metal-to-ligand stoichiometry. Furthermore, the synthesized complexes were also found to exhibit considerable antibacterial activity against both gram-positive and gram-negative bacteria, in addition to the above analytical reliability in the new luminol-based azo complexes. New metal complexes (CrII, CoII, and NiII) were constructed using novel ligands synthesized from the azo coupling reaction between luminol and sulfamethoxazole. Calibration curves for the λ_{max} were utilized to study the adherence of the complexes to the Beer-Lambert law.

1. Introduction

Luminol is a widely used compound in the field of chemiluminescence, often employed as a detection reagent for the presence of various oxidizing agents [1]. It has also been investigated for its potential biological activities. Synthesizing new complexes based on luminol and characterizing their properties can lead to the development of novel compounds with enhanced biological activities [2]. Azo compounds are characterised by stability [1], high selectivity [2] and sensitivity [3]. Therefore, they have been the focus of attention for researchers in the preparation of serious azo reagents [4–7]. Azo compounds have much importance in the commercial [8] and industrial

*Corresponding Author: Ban Khalil Ali

Email: ban.khlel@utq.edu.iq

https://doi.org/10.24200/amecj.v8.i03.1030

fields [9], since these are used to prepare thousands of azo dyes annually and are distinguished by their characteristic colour, especially red, orange, and yellow [10, 11]. They are also quick to prepare and have good performance [12]. Analytical studies on azo compounds [13–15] have proved their efficiency in quantitative and qualitative estimation, detection of elements and metal ions in low amounts [16], determination of the amount of formation of elements, especially transitional metals, flattening, extraction, and gel chromatography [17]. Luminol is a fluorescence reagent [18] used in analytical applications due to its efficient emission characteristics. Innovative nanomaterial-based sorbents, which have recently facilitated the extraction and determination of volatile organic compounds (VOCs), like toluene and BTEX, in environmental and food samples, include Teimoori et al, who reported on a toluene extraction-from-water-high-efficiency performance with aminopropyl trimethoxysilane-phenanthrene carbaldehyde-functionalized graphene oxide [19, 20]. Another study from the same group introduced functionalized multi-walled carbon nanotubes (MWCNTs) as rapid, dispersive micro-solid phase extraction capillaries to extract BTEX from water and milk [21]. High recoveries and low detection limits mark the achievement. Besides, nano-carbon structures have proven efficient in toluene extraction before GC analysis. Ashouri et al. contributed further by using ionic liquid-coated MWCNTs for the dynamic and static removal of benzene from air, as well as synthesizing carbon quantum dots from olive stones for efficient benzene adsorption [22, 23]. All of these reported studies appear to open up quite spectacular avenues for the functionalization of carbon nanomaterials and novel extraction techniques. This potential enables sensitive, rapid, and selective monitoring of hazardous organic pollutants in various matrices, as recently reviewed by Arjomandi et al. for heavy metal analysis in environmental and biological samples [24]. Recent studies have been conducted on VOC removal from different environmental matrices using other techniques. In their recent research, Mohammadi Asl et al [25] compared toluene removal from air using various methods. The study found that the ultraviolet semi-degradation-based adsorption process yielded significantly higher removal efficiency compared to adsorption alone for highly toluene-concentrated samples with extended contact times during the procedure. In a 2023 study conducted by Asl and Atabi [26], it was revealed that functionalized graphene oxide with bismuth and titanium oxide nanoparticles was excellent at removing formaldehyde from air by employing a dual photocatalytic degradation-adsorption mechanism, owing to its superior performance resulting from enhanced electron transfer and increased surface area compared to its traditional counterparts. Rakhtshah and Esmaeil [27] described the development of a novel microextraction technique utilizing ionic liquid-immobilized MWCNTs for the removal of styrene from water sample matrices. They achieved over 95% efficiency in extraction, along with good recoveries and detection limits in the rare μg L^{-1} range, compared to conventional methods, while drastically reducing processing time. In the same manner, Faghihi-Zarandi et al. [28] reported the efficiency of bismuth oxide in conjunction with heterogeneous graphene/graphene oxide in removing xylene vapor from the air by a combination of UV photocatalytic degradation and adsorption mechanism and showed that such hybrid material not only degraded the xylol into smaller fragments but also captured the intermediates giving the overall removal efficiencies higher than 85% under optimized conditions set for the experiment. Current studies are focused on preparing derivatives of luminol to increase their quantitative amounts by enhancing the colour intensity of luminol's ability to emit light upon oxidation [29]. Being a suitable reagent for azo formation with sulfamethaxadiazole and efficient, luminol is used in chemiluminescence [30] and bio-sensitization [31] processes. The effect of time, temperature, and pH stability, and its adherence to the Beer–Lambert law, has been demonstrated in spectroscopic studies using the prepared reagent. The bioavailability of sulfonamides against bacteria is due to their importance in treating various diseases [32, 33].

2. Experimental

2.1. Materials and instrumentation

All of the chemicals were of top quality. To measure the melting points of our compounds, we used a

Stuart SMP30 Melting Point Apparatus. We also used TLC for tracking our reaction. Then, we obtained spectral records using a Shimadzu UV-1650PC Spectrophotometer (Japan) and an FT-IR-8400S Shimadzu (Japan) to obtain infrared spectra with KBr pellets in the College of Science at the University of Dhi Qar. We used a Bruker DRX System AL 500 MHz Ultra Shield at Sanat Sharif University in Iran to obtain ^{1}H NMR spectra in the Chemistry Department. DMSO-d6 served as the solvent, and TMS was used as the reference. We sought to determine the electrical conductivity of the complex under laboratory-controlled conditions. We used an InoLab Cond 720 device (Xylem Analytics Company) with a platinum electrode, 10^{-3} molar concentration, and dimethyl sulfoxide solvent to measure the molar conductivity at room temperature. Ultimately, our testing revealed that the electrical properties of the complex are substantial. The reagents such as Luminol (5-Amino-2,3-dihydro-1,4-phthalazinedione, Sigma-Aldrich, USA, CAS No. 521-31-3), Sulfamethoxazole (Sigma-Aldrich, USA, CAS No. 723-46-6), Sodium nitrite ($NaNO_2$, Merck, Germany, CAS No. 7632-00-0), Sodium hydroxide (NaOH, Merck, Germany, CAS No. 1310-73-2), Hydrochloric acid (HCl, 37%: Merck, Germany, CAS No. 7647-01-0), Ethanol (absolute, Sigma-Aldrich, USA, CAS No. 64-17-5), n-Hexane (Sigma-Aldrich, USA, CAS No. 110-54-3), Ethyl acetate(Sigma-Aldrich, USA, CAS No. 141-78-6), Cobalt(II) chloride hexahydrate ($CoCl_2{\cdot}6H_2O$, Sigma-Aldrich, USA, CAS No. 7791-13-1), Nickel(II) nitrate hexahydrate ($Ni(NO_3)_2{\cdot}6H_2O$, Sigma-Aldrich, USA, CAS No. 13478-00-7), Chromium(III) chloride hexahydrate ($CrCl_3{\cdot}6H_2O$, Sigma-Aldrich, USA, CAS No. 10060-12-5), Deionized water(DW) Produced in-lab by Milli-Q water purification system, Potassium bromide (KBr) for IR (Sigma-Aldrich, USA, CAS No. 7758-02-3), Dimethyl sulfoxide-d6 (DMSO-d6, Sigma-Aldrich, USA, CAS No. 2206-27-1), and Tetramethylsilane (TMS, Sigma-Aldrich, USA, CAS No. 75-76-3) were used in this study, which were received as analytical chemicals without further purification, were utilized without further purification.

2.2. Preparation of azo dyes

A blend of 2.0 mL hydrochloric acid and 10 mL deionised water was stirred in a beaker, into which 0.01 moles of luminol had been dissolved. The temperature was cooled to between 0 and 5°C before a 0.01 M NaNO2 solution was added. After that, a 0.01 M solution of sulfamethoxazole dissolved in 5% NaOH was prepared, and the mixture was stirred for 2 hours. Finally, hot ethanol washed over it before it was recrystallized. We successfully prepared a brown precipitate using a 1:1 ratio of n-hexane and ethyl acetate. The reaction we tested had an Rf value of 0.65, and its melting point was 287-288°C. You can take a gander at the diagram (Scheme 1) to get a better idea of the process [34], while Table 1 offers up some physical characteristics and elemental analyses.

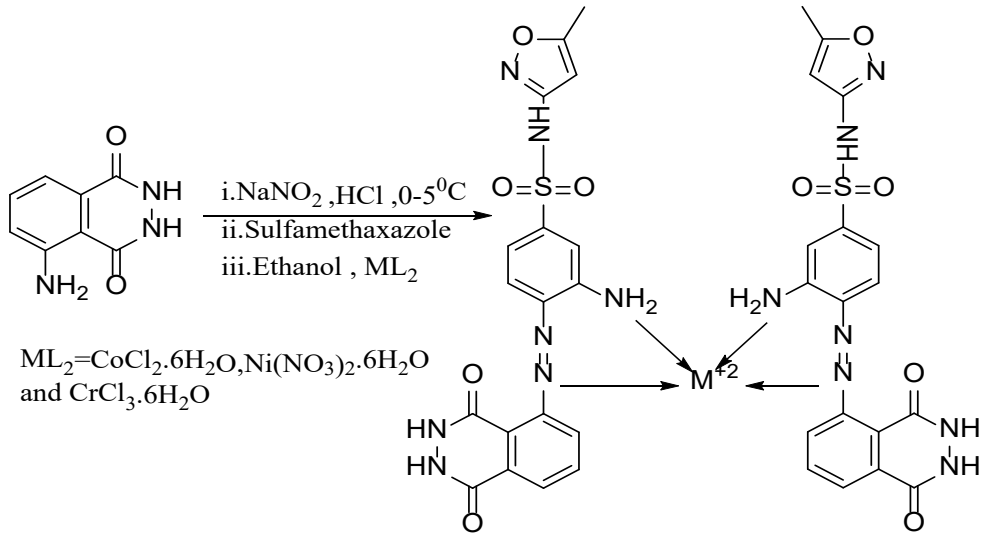

Scheme 1. Synthesis of azo compounds

Table 1. Physical properties and novel azo dyes and compounds

No	Complexes	M.Wt	Colour	m.p°C	Yield%
1	azo dyes	441	Brown	287-288	85
2	[Cr (L) $(H_2O)_2$] Cl_2	707.45	Light brown	272-274	68
3	[Co (L) $(H_2O)_2$] Cl_2	731.97	Dark brown	296 -298	79
4	[Ni (L)] $(NO_3)_2$	678	Black	263-264	77

2.3. Preparation of metal complexes

To prepare our azo-azomethine complex, we began by dissolving 0.005 mole of the ligand in hot ethanol. Then, we carefully added 0.005 moles of $CoCl_2$ · 6H2O, $Ni(NO_3)_2 \cdot 6H_2O$, and CrCl3 · 6H2O, each in a 1:1 molar ratio, to a pH-adjusted solution made from a 0.05 M HCl and 0.05 M NaOH mixture. All solutions were in 20 mL of liquid for each metal, adjusted to the optimal pH for each component. Finally, we set our mixture to simmer between 30-45°C for about 12–15 hours, until a solid precipitate formed. Separate the mixture by filtration, and then give it several hot washes with 10 mL of ethanol. Finally, dry for a moment before fully re-crystallizing using absolute ethanol [35].

2.4. Preparation of Solutions

The standard solutions of metal ions were prepared. The weights of (0.118, 0.085, and 0.068 g) of $CoCl_2.6H_2O$, $Ni(NO_3)_2.6H_2O$, and $CrCl_3.6H_2O$ were dissolved into a 100 mL solution of distilled water, diluting them until complete. Sodium hydroxide (0.05M) solution was made by melting 0.5 g of material in a beaker, then transferring it to a volumetric flask and diluting it with deionized water up to the mark. Hydrochloric acid (0.05M) solution prepared by adding 1.036 ml of concentrated HCl solution (d=1.19 g mL^{-1}, 37% w/w) slowly with stirring to an appropriate amount of distilled water in a 250 ml volumetric flask, and complete the volume up to the mark with distilled water. The solution of 1 × 10^{-3} for spectrophotometry was prepared by adding 1 mL of the ion concentration solution (100 µg mL^{-1}) into a 10 mL volumetric flask, along with 2 mL of reagent (1×10^{-3} M). Once the metal ions that react to the reagent have been determined, determine λ_{max} and fill the flask to the mark with deionized water. For the blank solution, prepare it in the same manner, but omit the ion under study (Scheme 2).

2.5. Method of conducting spectral studies

2.5.1. The effect of reagent volume

At λ_{max}, the absorbance of metal-chelates was recorded by shaking well the reagents of various volumes (0–3 mL) at a concentration of 1×10^{-3} M with 1.0 mL of metal ion solutions. This was done against a prepared reagent blank.

2.5.2. The effect of reaction time

1.0 mL of metal ion solutions at a concentration of 1×10^{-3} M was shaken well to study the effect of time on the stability of the complexes at the optimal size. The absorption of metal-chelates was then recorded at λ_{max} (0-70) min against the prepared reagent blank.

2.5.3. Effect of pH value

The absorption of complexes at various pH levels was investigated by using HCl and NaOH solutions. Metal ion solutions 1.0 mL concentration 1×10^{-3}M were mixed with the appropriate reagent volume at different pH values ranging from 2 to 12. The absorbance was then measured at the suitable λ_{max} against a blank prepared with the reagent. Additionally, 0.05 M concentrations of HCl and NaOH solutions were utilized in this experiment.

2.5.4. Effect on temperature

Placing 1mL of metal ion solutions, we then studied the effect of temperature on reagent concentration

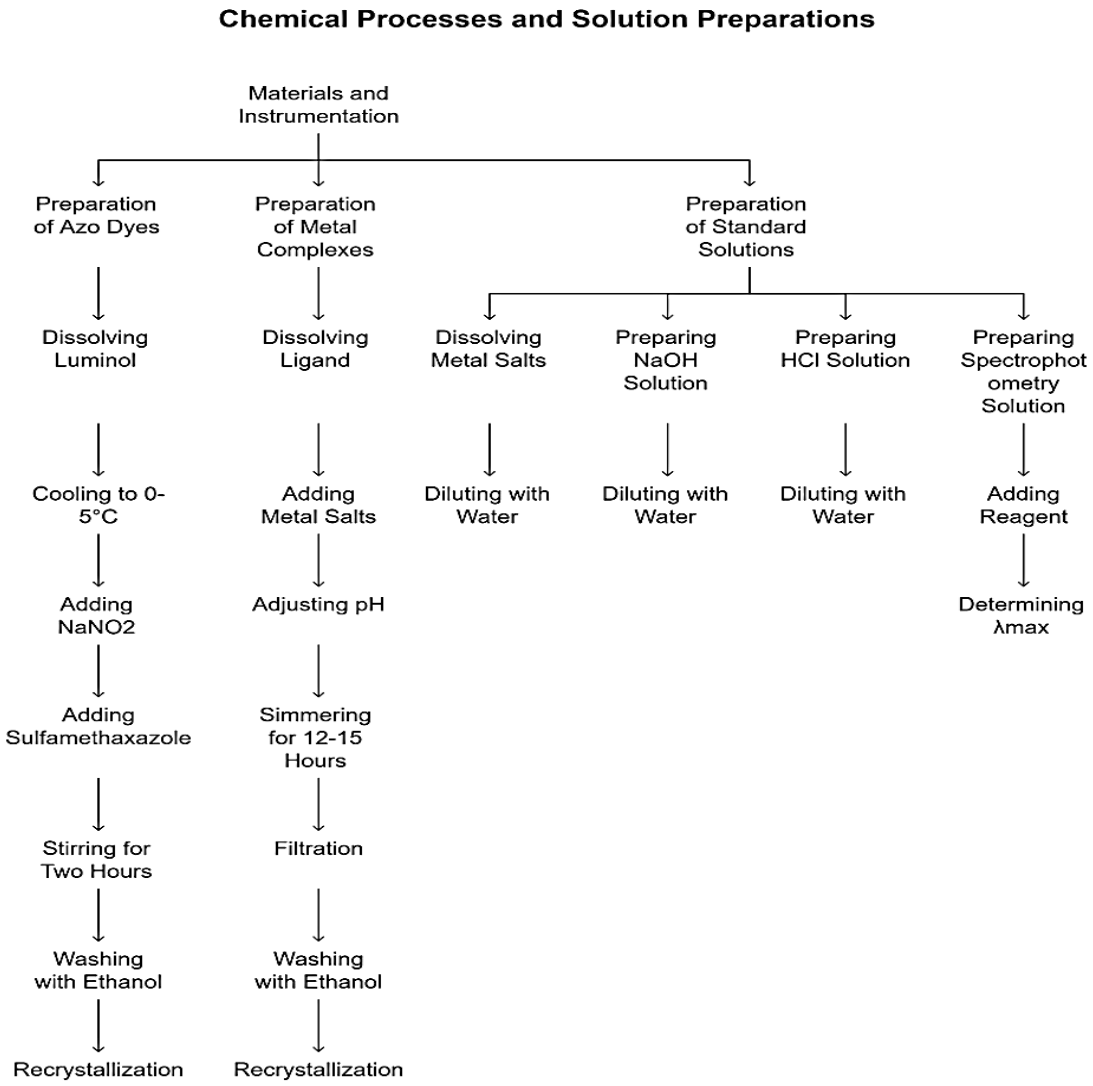

Scheme 2. Chemical process and solutions preparation steps

1×10^{-3} M by adjusting the pH and immersing it in a water bath with varying temperatures (0 - 80) ºC. After the optimal time, we measured the absorbance at the appropriate λ_{max} against a prepared reagent blank.

2.6. Determination of degree of dissociation and stability constant

We took equivalent volumes of the reagent and metal ion solutions at 1×10^{-4} M, and the stability constant of the complexes was measured. The absorption at λ_{max} and optimal pH values was also measured. The ideal state for each complex was adopted for the measurement. To calculate the dissociation degree and stability constant, the (Am and As) value was measured against a reagent blank. This value represents the complex in partial dissociation. The experiment was then repeated with an excessive volume of reagent. The absorbance of the complexes at the appropriate λ_{max} was measured against a reagent blank prepared without ions. This measurement represents the non-dissociation complex. The interaction between the metal ions and reagents can be represented by the following Equation 1.

$$\propto = \frac{A_m - A_s}{A_m} \qquad \text{(Eq.1)}$$

2.7. Determination of the stoichiometry of the complex

The continuous variation method and the Molar ratio method were used. The variation method involved in this experiment required the careful combination of solutions containing metal ions and ligands. These solutions were prepared with equal molar concentrations of 1×10^{-4} M but variable volumes of solution. The total volume of the combined solutions remained constant at 2 ml. After mixing, the absorbance of each solution was measured at its respective λ_{max}. Additionally, in the Molar ratio method, the total volume remained constant at 2 mL, and the ligand concentration was maintained at 1×10^{-4} M. The metal ions varied in concentration. Next, the absorbance of each solution was measured at λ_{max}.

2.8. Biological activity

At the Biology Department of the University of Dhi Qar, we examined the biological activity of the complex utilizing the diffusion agar method. Our focus was on positive and two types of harmful gram bacteria, specifically Staphylococcus aureus, E. coli, and K. pneumoniae, which were diseased isolates. To assess the inhibitory effect of the complex, we created three holes in the cultured spectra and inserted the prepared complex. The cultivars grown with bacteria were exposed to four different concentrations of the complex before being placed in an incubator at 37 °C for 24 hours. The measurement of the inhibition zone was then conducted for each case [36].

3. Results and Discussion

3.1. UV-Vis spectra

We logged the UV-VIS spectrum of azo-azomethine dyes using Figures 1(a-d). Once dissolved in DMSO at room temperature in the range (200-800) nm, the concoction emitted two notable absorptions: one ranging from 238-325 nm concerning transitions from π→π* in the aromatic ring, and another situated between 400-470 nm attributed to (n→π*) paired with (-C=N-) and (-N=N-) bonds [37] (Table 2).

Table 2. Electronic spectrum and magnetic moment of the complex

No	Complexes	λ_{max}	Transition	Suggested geometry
1	azod yes	305, 356	n→π*, π→π*	-
2	[Cr (L) $(H_2O)_2$] Cl_2	297, 354, 450	n→π*, π→π*	Octahedral
3	[Co (L) $(H_2O)_2$] Cl_2	300, 386, 439	n→π*, π→π*	Octahedral
4	[Ni (L)] $(NO_3)_2$	321, 350, 409, 476	n→π*, π→π*	Tetrahedral

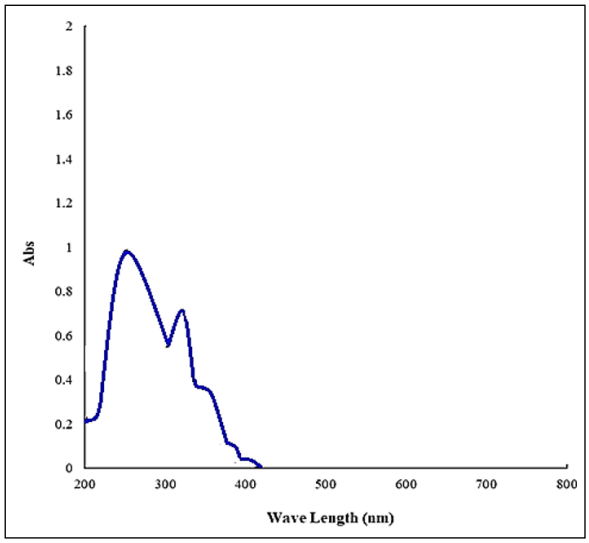

Fig. 1a. UV-Vis spectra of azo dyes

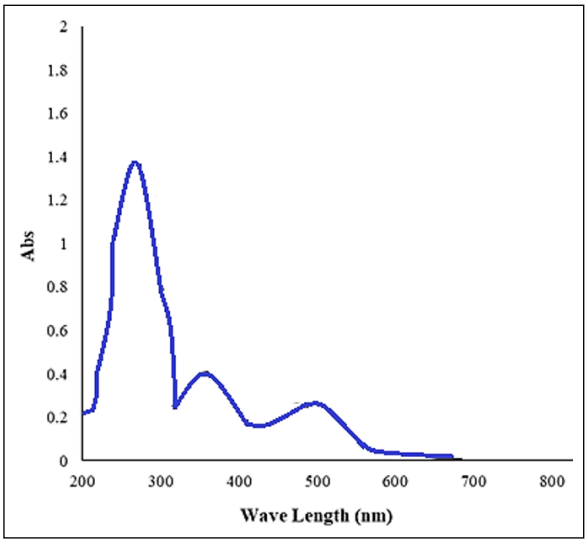

Fig. 1b. UV-Vis spectra of $[Cr(L)(H_2O)_2]Cl_2$

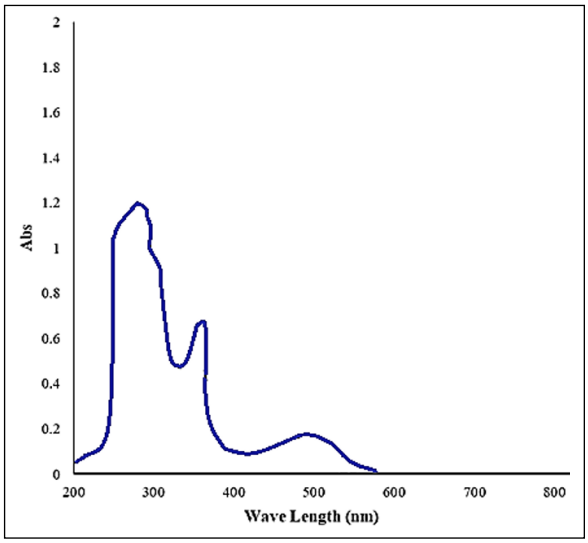

Fig. 1c. UV-Vis spectra of $[Co(L)(H_2O)_2]Cl_2$

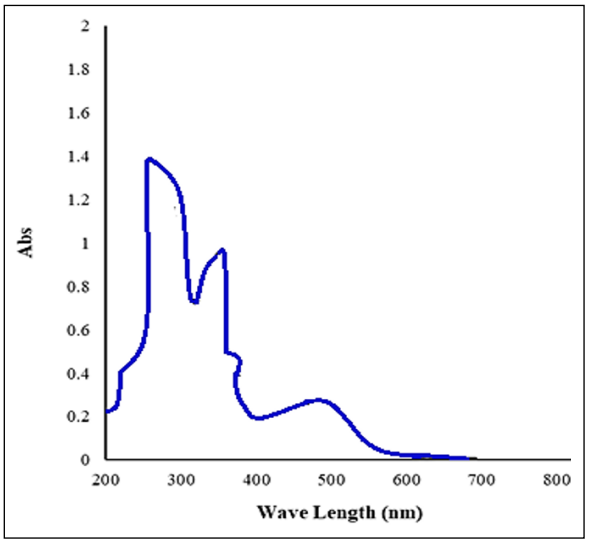

Fig. 1d. UV-Vis spectra of $[Ni(L)](NO_3)_2$ complex

3.2. FT-IR spectra of ligand

Using a Shimadzu FT-IR spectrophotometer, the azo-azomethine ligand's IR spectrum was acquired with a KBr disk. The obtained spectrum, displayed in Figure 2, revealed peaks at 3460-3416 for (NH2), 3322 for (NH), 3004 for (C-H oxazole ring), 2905 for (C-H aromatic), 1652 for (C=O amide), 1590 for (C=C), and 1440 for (C-O) [1, 38].

3.3. ^{1}H-NMR spectrum

Figure 3 displays the ^{1}H-NMR spectrum of the azo-azomethine, prepared at 400 MHz with DMSO-d6. This spectrum reveals the following peaks: 14.09 (s, 0H), 13.27 (s, 1H), 11.48 (s, 2H), 8.19 (d, J = 8.3 Hz), (1H), 8.14–8.04 (m, 0H), 8.00–7.92 (m, 1H), 7.96–7.81 (m, 5H), 7.66 (d, J = 10.1 Hz, 4H), 7.48 (t, J =7.9 Hz, 2H), 6.95 (dd, J=22.5, 7.9 Hz, 3H), 6.20 (d, J = 8.2 Hz, 2H), and 11.58 (s, 0H)[1].

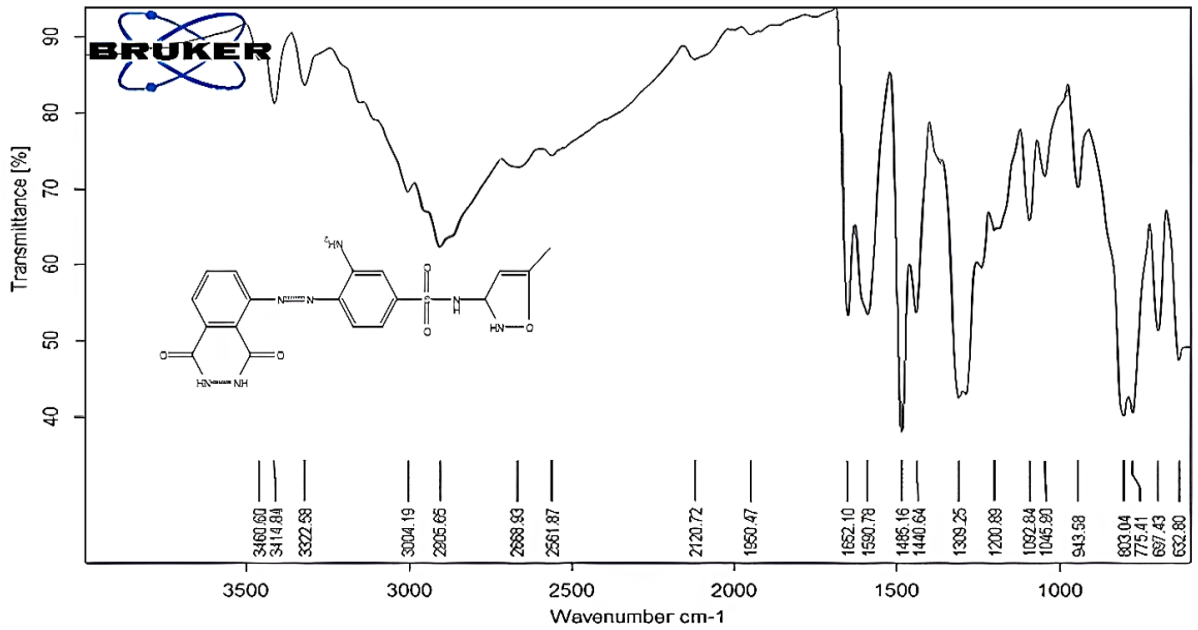

Fig. 2. FT-IR spectra of prepared ligand

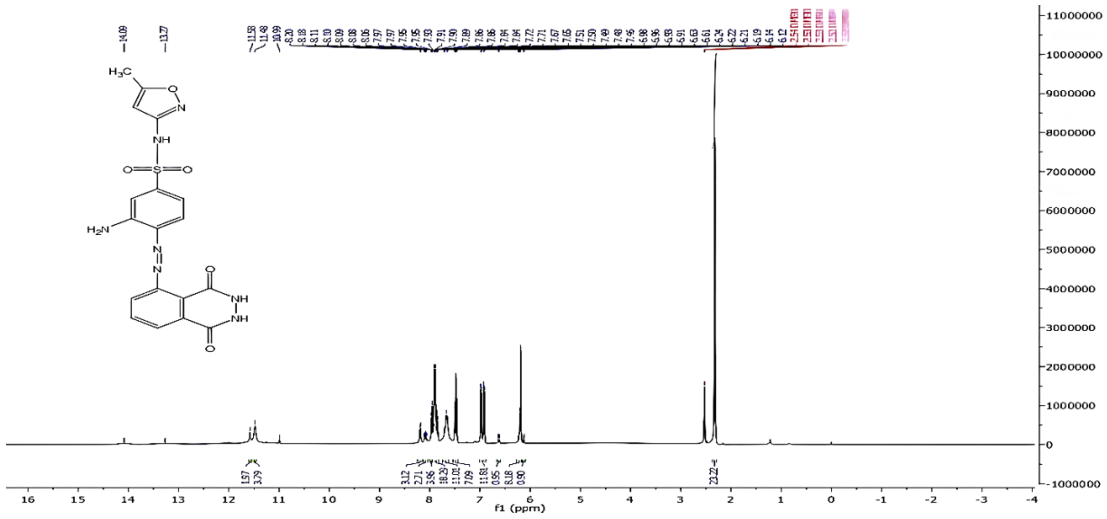

Fig. 3. ^{1}H-NMR of prepared ligand

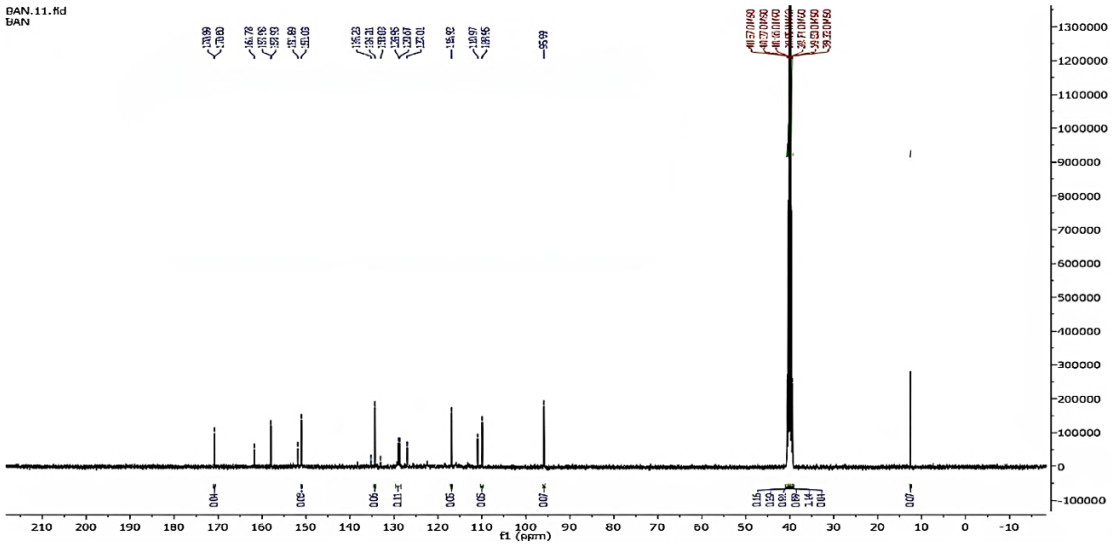

Fig. 4. ^{13}C-NMR of prepared ligand

3.4. ^{13}C-NMR spectrum

^{13}C-NMR spectrum of ligand followed by (101 MHz, DMSO-D6) δ 170.80, 161.78, 157.98, 157.93, 151.89, 151.03, 135.23, 134.31, 133.03, 128.67, 127.01, 116.95, as shown in Figure 4.

3.5. Experimental condition optimization

3.5.1.Effect of reagent volume

The adsorption at λ_{max} was recorded by studying the effect of the detector. Different volumes (0-3 mL) of the reagent (1×10^{-3} M) were used with 1.0 mL of metal Ni(II), Co(II), and Cr(II), showing the highest absorbance with 1-2 mL of the reagent. Figure 5 displays the results.

3.5.2.Effect of reaction time

It is essential to determine the time during which the compound maintains its stability, and the study was conducted over a period of 0-70 minutes. The components were mixed at room temperature, and the reaction remained stable for 24 hours, indicating a potent coordination ligand with metal ions. Figure 6 displays the results.

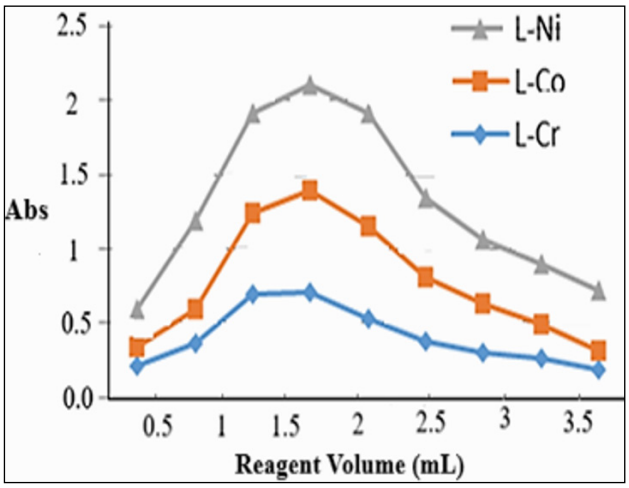

Fig. 5. Effect of volume at λ_{max} for complexes

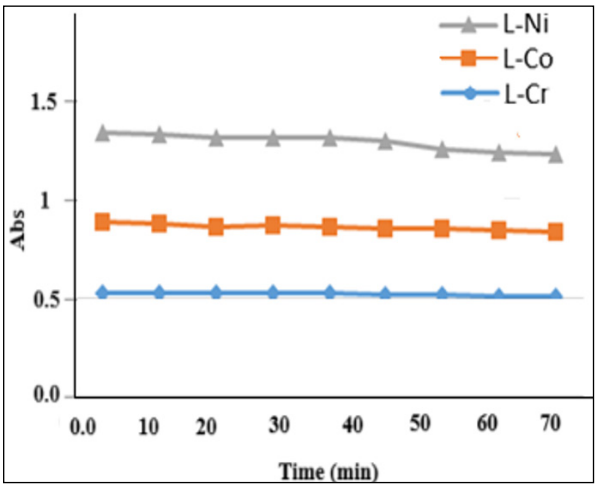

Fig. 6. Effect of time at λ_{max} for complexes

3.5.3. Effect of pH

The ion complexes measured at λ_{max} exhibit changes in absorbance relative to solution pH. Initially, the absorbance of each complex is low on the acidic side and gradually increases until it reaches its maximum at the ideal pH value. Subsequently, as the pH increases, the absorbance decreases. The charts indicate that the optimal pH values for L-Cr, L-Co, and L-Ni are 10, 8, and 7, respectively. These chelate complex solutions remain stable within a pH range of 6-10. The observed decrease in absorbance can be attributed to the high proton content of the ligand at lower pH levels. This abundance of protons inhibits the formation of complexes by preventing electron pairs from bonding with the metal cations. Figure 7 displays the results.

3.5.4. Temperature effect

The complex was studied for its temperature effect from 10 to 80 degrees Celsius. The appropriate temperature range for complex formation was found to be between 30 and 45 degrees Celsius, as indicated by the maximum absorbance shown in Figure 8. However, as the temperature increased, the complex started to dissociate, leading to a decrease in absorbance [39].

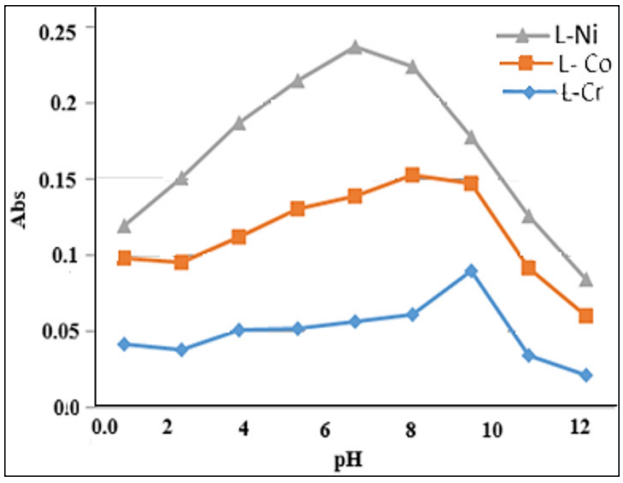

Fig. 7. Effect of pH on complexes

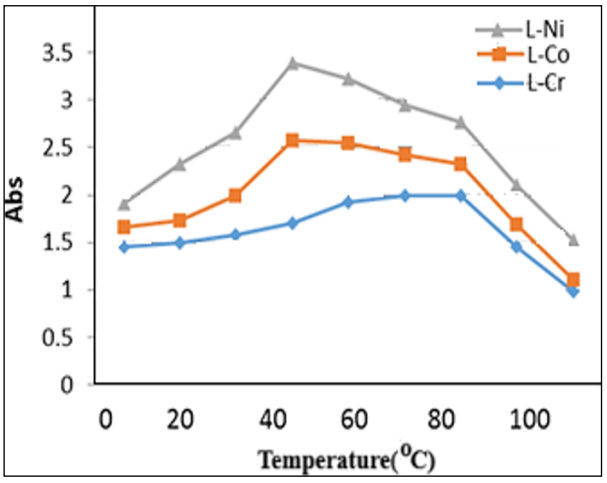

Fig. 8. Effect of temperature on complexes

3.6. Determination of complex stoichiometry

We solved the complex stoichiometry using a technique called Joppe's continuous variation method. To make it happen, we created an assortment of solutions that all had the same molar concentration of metal and ligand. Next, we jotted down the absorbance at λ_{max}. Afterward, we assessed the mole fraction of $Vm/(Vm+VL)$ for the X-axis; Vm and VL are abbreviations for volumes of metal and ligand, respectively. Lastly, we plotted all the absorbance values on the Y-axis. We discovered that the M:L ratio for all complexes was an even 1:1. To double-check our work, we put the molar ratios method to the test and still ended up with the same result. Visualizing this through plotting absorption values on the Y-axis and CL/CM on the other, where CL and CM designate concentration of metal and ligand solutions, respectively, showed a slight variance from a straight line at a strict 1 value. This is best visualized in Figure 9, which covers both methods [39].

3.7. Beer's law

To estimate complex spectra, the Beer-Lambert law was studied on solutions of complexes with ligands. The absorbance was recorded at λ_{max}, and it represents the sensitivity of the method through the calibration curve defined by the molar absorption coefficient**.** The calculation of various values, such as (ε_{max}), through the slope curve, which is represented by Equation 2.

$$\text{Slope} = \sum [(X-X_A)(Y-Y_A)] / \sum (X-X_A)^2$$
$$r = \sum [(X-X_A)(Y-Y_A) / [(\sum (X-X_A)^2)(\sum (Y-Y_A)^2)]^{1/2}$$

(Eq.2)

The following constants are: X = concentration values, X_A = concentration rate, Y = absorption values, and YA = absorption rate. Also, the specific absorbance (a) is defined in terms of molar absorption as in the following Equation 3.

$$a = \varepsilon / (At.Wt \times 1000) \quad \text{(Eq.3)}$$

Sandell sensitivity (S) for complexes represents the number of micrograms of the substance to be determined per millilitre of solution, with an absorption value of 0.001 in its display cell 1 cm, as it expresses µg cm^{-2} (Eq. 4).

$$S = 10^{-3} / a \quad \text{(Eq.4)}$$

Through an equation, standard deviation (S.D), the following constants are: X = average readings absorbance values, N = the number of laboratory readings, X_1 = the value of each laboratory reading, while the relative Standard deviation percentile (Equations 5 and 6). The data is shown in Table 3.

$$S.D = [(\sum (X_1-X^-)^2/(N-1)]^{1/2} \quad \text{(Eq.5)}$$

$$D.L = 3 \times S.D \text{ of blank} / \text{slope} \quad \text{(Eq.6)}$$

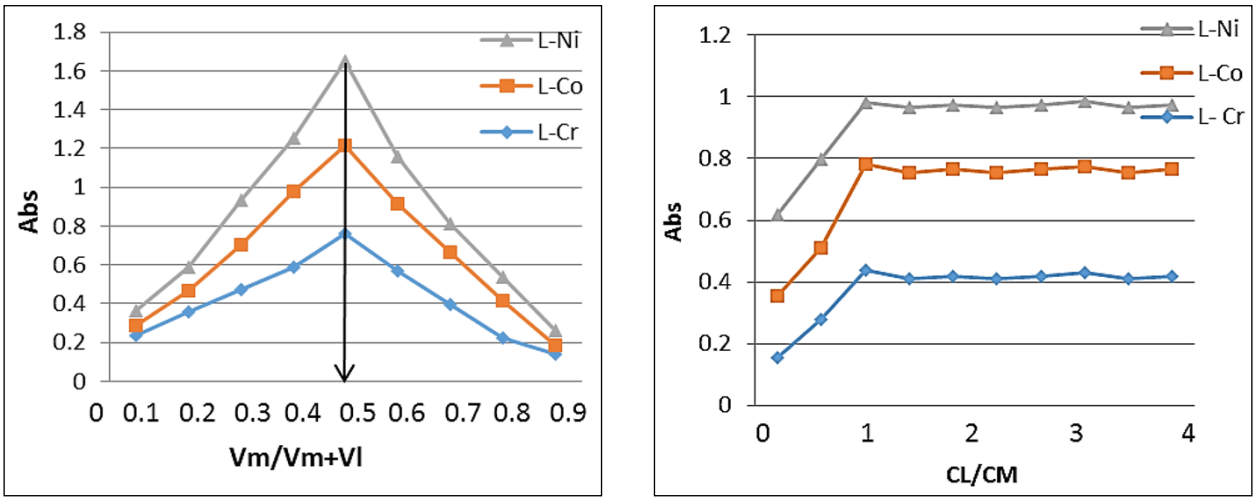

Fig. 9. The Job's method (left) and the continuous variation method (Right) measure the formed product complex at λ_{max}

Table 3. Beer's law data, as well as the sensitivity and precision of the complexes

Complexes	λ_{max} (nm)	ε_{max} ($\varepsilon\times 10^4$)	a mL $(g\times cm)^{-1}$	S ($\mu g\ cm^{-2}$)	R^2	SD	DL $x10^{-5}$ ($\mu g\ mL^{-1}$)
[Cr (L) $(H_2O)_2$] Cl_2	450	0.72	0.114	0.009	0.99	0.09	0.029
[Co (L) $(H_2O)_2$] Cl_2	439	0.25	0.023	0.042	0.99	0.93	0.282
[Ni (L)]$(NO_3)_2$	476	0.58	0.026	0.038	0.99	0.13	0.071

3.8. Calculation stability constant (K_s) of the metal complexes

We were able to work out the stability constant (K) of metal ions with complexes by plugging their info into this equation (Eq.7). To do this, we measured the absorbance of their solutions at a specific wavelength and pH level,

$$K = \frac{1-\propto}{4\propto^3 c^2} \qquad \text{(Eq.7)}$$

Where c is the concentration of the complex solution given in mol L^{-1}.

The facts of our findings align perfectly with the Irving-Williams series [40]. It offers stability and insight into how secure the compound. There is a level of fragmentation, as noted in the math, that is supported by Table 4. Interestingly, we observed that the concentration of this complex solution influences its K value, reflecting its remarkable strength.

3.9. Molar electrical conductivity

The relationship between the amount of ions released by a complex in a solution and the degree of electrical conductivity is determined by the ionic formula, which can be identified through the measurement of electrical conductivity. This measurement is based on the quantity of solute in a $1cm^3$ solution and is essential in understanding the complexity of compounds in solutions, as shown in Equation 8.

$$\text{L complex} = \text{A solution} - \text{A solvent}$$
$$\text{K} = \text{L complex} \times \text{K cell}$$
$$\wedge\text{m} = 1000\ \text{K/C}$$

(Eq.8)

Cell constant (K cell) is equal to the complex conductivity (L complex) divided by the solution conductivity (A solution) and the solvent conductivity (A solvent). Specific conductance (K) is equal to the product of the molar concentration (C) and the molar conductivity (∧m).

Our laboratory is analyzing the molar conductivity of real-world complex solutions. We added azo dyes to test compounds with Cr(II), Co(II), and Ni(II) ions, dissolved in DMSO at 10^{-3} M concentration. To have something to compare our findings with, we also tested how distilled water reacted. After all was said and done, we determined that the complexes behaved like ionic compounds, with a 1:2 ratio

Table 4. Stability constants of the prepared complexes

Complexes	As	Am	α	k	Log k
[Cr (L) $(H_2O)_2$] Cl_2	0.542	0.532	0.0184	2.8×10^{11}	46.08
[Co (L) $(H_2O)_2$] Cl_2	0.536	0.522	0.0261	1.42×10^{11}	15.22
[Ni (L)]$(NO_3)_2$	0.558	0.534	0.8569	1.94×10^{11}	28.78

depending on the presence of chloride and nitrate ions outside the coordination sphere. If you introduce silver nitrate ($AgNO_3$) to the mixture, you'll start to see some white residue. That's a clear indication that chloride particles are outside the sphere of influence, increasing in number in proportion to the presence of chlorides (Table 5) [41, 42].

3.10. Analysis of different concentrations of luminol by UV-Vis

To calibrate the luminol-based method and check its linearity, luminol solutions at varying concentrations (1, 2, 5, 10, 15, and 20 mg L^{-1}) were prepared and measured by absorbance at the characteristic λmax, identified in the spectra to occur between 300 and 400 nm for luminol derivatives. The results are summarized in Table 6. Luminol quantification via UV-Vis is highly sensitive and accurate, with good precision over a wide concentration range. The successful spike recovery experiments support the conduct of real sample analysis and robustness against possible matrix effects. This validates the luminol-based method for both analytical and complexation studies, as demonstrated by the spectra shown.

3.11. Antibacterial activity

According to Figure 10, the antibacterial activity results of the complex under study indicate that when dissolved in dimethylsulfoxide, its effect on Gram-positive bacteria (S. aureus) is greater than on the other two types. The highest inhibition zone (16) was observed at a concentration of 125 µm. In comparison, the lowest (9) was recorded at a concentration of 25 µm, suggesting the high efficacy of S. aureus bacteria in lipid penetration and biofilm production [43].

Table 5. Molar electrical conductivity of the prepared complexes

No	Complexes	^m (S cm^2 $mole^{-1}$) in DMSO	Electrolyte Type
1	[Cr (L) $(H_2O)_2$] Cl_2	75	1:2
2	[Co (L) $(H_2O)_2$] Cl_2	78	1:2
3	[Ni (L)]$(NO_3)_2$	77	1:2

Table 6. Validation based on spike Luminol and analysis by UV-Vis

Sample	Added (mgL^{-1})	Absorbance (λ_{max})	Found (mgL^{-1})	Recovery (%)	RSD (%)
DW	2	0.31	2.04	101.2	2.1
DW	5	0.735	4.92	98.3	1.8
DW	10	1.48	9.85	98.0	2.3
DW	15	2.21	14.7	98.1	2
DW	20	2.95	19.6	98.2	1.7
Luminol	-----	0.34	2.21	-----	1.9
	2	0.605	4.16	97.5	2.4
Luminol	-----	0.33	2.19	-----	2.1
	3	0.728	5.11	97.3	1.8

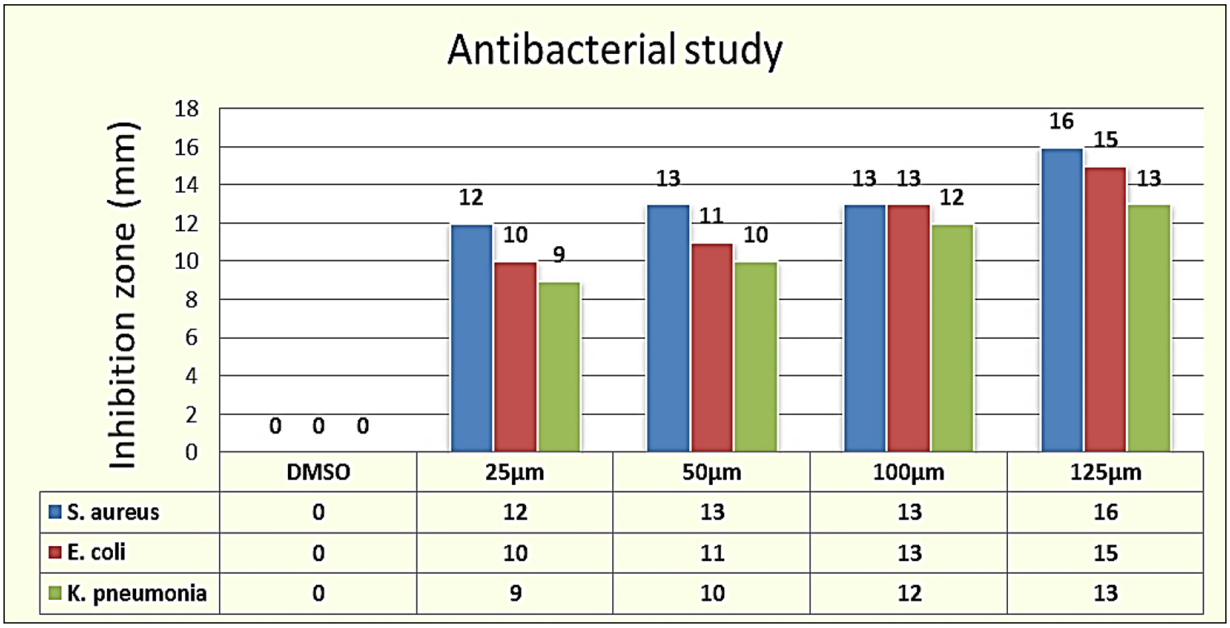

Fig. 10. Antibacterial activity of prepared complexes

4. Conclusions

In this study, the new complexes of luminol, a chemiluminescent material, were analyzed for biological activity using spectroscopic methods. According to spectral analysis and the suggested structural formula, it can be concluded that the ligand coordinates primarily through the two mentioned nitrogen atoms with metal ions, confirming the existing chelation mode. The molar ratio method consistently demonstrated a one-to-one stoichiometric relationship between the ligand and metal ions in all the complexes. The complexes had maximum formation under alkaline conditions, clearly showing the significance of pH in the process of synthesis. Kinetic studies indicated that the complexes remained stable over time, which agrees very well with the calculated degree of dissociation and the very high stability constants, thus establishing the stability factor. Biological assays demonstrate that the ligand and its metal complexes exhibit significant antibacterial activity against Escherichia coli, Staphylococcus aureus, and Klebsiella pneumoniae, suggesting potential antimicrobial applications. The reproducibility of the findings was confirmed by relative standard deviations of less than 3% and recovery rates ranging from 97% to 102%, indicating the reliability and accuracy of the experimental procedures.

5. Acknowledgment

The author declares that they have no known competing financial interests or personal relationships that could have appeared to influence the work reported in this paper

6. References

[1] H.W. Gao, J.F. Zhao, Stability constants of cobalt(II) and copper(II) complexes with 3-[(o-carboxy-p-nitrobenzene) azo] chromotropic acid and selective determination of copper(II) by competition coordination, Croatica Chem. Acta, 76 (2003) 1–6. https://hrcak.srce.hr/file/151616

[2] I. Talib Humeidy, Spectrophotometric method for determination of sulfamerazine using 2,4-dinitrophenylhydrazineReagent, J. Phys.: Conf. Ser., 1294 (2019) 052022. https://doi.org/10.1088/1742-6596/1294/5/052022

[3] A. Mittal, V. Thakur, J. Mittal, H. Vardhan, Process development for the removal of hazardous anionic azo dye Congo red from wastewater by using hen feather as potential adsorbent, Desalin. Water Treat., 52 (2014) 227–237. https://doi.org/10.1080/19443994.2013.785030

[4] A.M.M. Tayib, Synthesis and characterization Of Metal ions complexes of Mn (II), Fe (II),

Co (II), Ni (II), Cu (II) and Zn (II) with mixed ligands of 2 aminopyrimidine dithiocarbamate and diamine, World J. Pharm. Pharm. Sci., 10 (2021) 2620-2632. https://doi.org/ 10.20959/ wjpps20218-19737

[5] M.R. Abd-Alzahra, Z.M. Hatem, N.Q.A. Maged, I.K. Kareem, Synthesis and characterization of novel metal complexes with new azo-schiff base ligand derived from sulfa drug and toxicological studies of its complexes as antibacterial, Int. J. Health Sci., 6 (2022) 5524–5539. https://doi.org/ 10.53730/ ijhs. v6nS1.5654

[6] A.N.M.A. Alaghaz, H.A. Bayoumi, Y.A. Ammar, S.A. Aldhlmani, Synthesis, characterization, and antipathogenic studies of some transition metal complexes with N,O-chelating Schiff's base ligand incorporating azo and sulfonamide Moieties, J. Mol. Struct., 1035 (2013) 383–399. https:// doi.org/ 10.1016/ j.molstruc.2012.11.030

[7] K.K. Mehta, S.T. Patel, A.D. Patel, Studies on chelating properties of antipyrine based azo ligands and its coordination compounds, Der Pharm. Chem., 9 (2017) 79–82. https:// www.derpharmachemica.com/

[8] M. Hosseinkhani, H. Shirafkan, Usage of cotton fabric substrate for synthesis mono azo dye, Res. J. Pharm. Biol. Chem. Sci., 6 (2015) 494–501. https://www.rjpbcs.com/archives.html

[9] A. J. Jarad, Synthesis and characterization of new azo dye complexes with selected metal ions, J. Al-Nahrain Uni. Sci., 15 (2012) 74–81. https://doi.org/10.22401/jnus.15.4.09

[10] H. Langhals, Color Chemistry: synthesis, properties and applications of organic dyes and pigments, 3rd revised edition, By Heinrich Zollinger, Wiley book, Angewandte Chemie International Edition, 43 (2004), 5291–5292. https://doi.org/10.1002/anie.200385122

[11] S. M. Benkhaya, S. rabet, A. El Harfi, A review on classifications, recent synthesis and applications of textile dyes, Inorg. Chem. Commun., 115 (2020) 107891. https://doi.org/10.1016/j.inoche.2020.107891

[12] J. Levita, S. Megantara, M. Mutakin, Photometric titration method to determine bromination of red and yellow dyes in crackers, Int. J. Chem., 4 (2012) 80. https://doi.org/ 10.5539/ ijc.v4n3p80

[13] A.A. Ali, T.A. Fahad, A.A. Al-Muhsin, Preparation and spectroanalytical studies of two new azo dyes based on Luminol, IOP Conf. Ser.: Mater. Sci. Eng., 928 (2020) 52007. https://doi.org/ 10.1088/ 1757-899X/ 928/ 5/ 052007

[14] P. Nagaraja, S.D. Naik, A.K. Shrestha, A. Shivakumar, A sensitive spectrophotometric method for the determination of sulfonamides in pharmaceutical preparations, Acta Pharm., 57 (2007) 333–342. https://doi.org/10.2478/ v10007-007-0026-4

[15] M.A. Grimminger, M.P. Tracey, S.J. Martinus, Colorful approach to teaching extraction using Aazo dyes and comparison of hands-on vs distance learning assessment, J. Chem. Educ., 98 (2021) 3509–3513. https://doi.org/10.1021/acs.jchemed.1c00465

[16] S. Serin, M. Kurtolu, Potentiometric titrations of some azo dyes containing a hydroxy group with tetrabutylammonium hydroxide in acetonitrile, Analyst, 119 (1994) 2213–2215. https://doi.org/10.1039/AN9941902213

[17] Y. Chen, L. Zhang, L. Feng, G. Chen, Y. Wang, Z. Zhai, Q. Zhang, Exploration of the key functional strains from an azo dye degradation microbial community by DGGE and high-throughput sequencing technology, Environ. Sci. Pollut. Res., 26 (2019) 24658–24671. https://doi.org/10.1007/s11356-019-05781-z

[18] A.K. Abd, L.A.R. Al-Iessa, Synthesis and Spectral Properties of some new derivatives of Luminol azo dyes, J. Kufa Chem. Sci., 2 (2020) 47–60. https://journal.uokufa.edu.iq/ index.php/jkcs/article/view/11039

[19] S. Teimoori, A. H. Hassani, M. Panahi, N. Mansouri, An immobilization of aminopropyl trimethoxysilane-phenanthrene carbaldehyde on graphene oxide for toluene extraction and separation in water samples, Chemosphere, 316 (2023) 137800. https://doi.org/10.1016/j.chemosphere.2023.137800

[20] S. Teimoori, A. H. Hassani, M. Panahi, N.

Mansouri, Rapid extraction of BTEX in water and milk samples based on functionalized MWCNTs by dispersive homogenized-micro-solid phase extraction, Food Chem., 421 (2023) 136229. https://doi.org/10.1016/j.foodchem.2023.136229

[21] S. Teimoori, A. H. Hassani, New extraction of toluene from water samples based on nano-carbon structure before determination by gas chromatography, Int. J. Environ. Sci. Technol., 20 (2023) 6589–6608. https://doi.org/10.1007/s13762-023-04906-9

[22] R. Ashouri, N. Mansouri, Dynamic and static removal of benzene from air based on task-specific ionic liquid coated on MWCNTs by sorbent tube-headspace solid-phase extraction procedure, Int. J. Environ. Sci. Technol., 18 (2021) 2377-2390. https://doi.org/10.1007/s13762-020-02995-4

[23] R. Ashouri, S. A. Hajiseyed Mirzahosseini, N. Mansouri, Synthesis of carbon quantum Dots from olive stones for efficient adsorption of benzene from the ambient air, J. Nanostruct., 11 (2021) 480-497. https://doi.org/10.22052/JNS.2021.03.007

[24] M. Arjomandi, A review: analytical methods for heavy metals determination in environment and human samples, Anal. Methods Environ. Chem. J., 2 (2019) 97-126. https:// doi.org/10.24200/amecj. v2.i03.73

[25] M. Mohammadi Asl, N. Mansouri, S. A. R. Haji Seyed Mirzahosseini, F. Atabi, Simultaneity comparative evaluation of toluene removal from the air by adsorption and UV semi-degradation-based adsorption procedure, Int. J. Environ. Sci. Technol., 21 (2024) 6677-6694. https://doi.org/10.1007/s13762-024-05503-0

[26] M. Mohammadi Asl, F. Atabi, Functionalized graphene oxide with bismuth and titanium oxide nanoparticles for efficiently removing formaldehyde from the air by photocatalytic degradation–adsorption process, J. Anal. Test., 7 (2023) 444-458. https:// doi.org/ 10.1007/s41664- 023-00272-0

[27] J. Rakhtshah, N. Esmaeil, A rapid extraction of toxic styrene from water and wastewater samples based on hydroxyethyl methylimidazolium tetrafluoroborate immobilized on MWCNTs by ultra-assisted dispersive cyclic conjugation-micro-solid phase extraction, Microchem. J., 170 (2021) 106759. https:// doi.org/ 10.1016/j.microc. 2021.106759

[28] A. Faghihi-Zarandi, J. Rakhtshah, B. B. Yarahmadi, A rapid removal of xylene vapor from environmental air based on bismuth oxide coupled to heterogeneous graphene/graphene oxide by UV photo-catalectic degradation-adsorption procedure, J. Environ. Chem. Eng., 8 (2020) 104193. https:// doi.org/ 10.1016/j.jece.2020.104193

[29] S. Deepa, S.R. Reddy, K. Rajendrakumar, Green chemiluminescence of highly fluorescent symmetrical azo-based luminol derivative, Orient. J. Chem., 34 (2018) 894–905. https:// doi.org/ 10.13005/ ojc/340238

[30] C. Zhao, H. Cui, J. Duan, S. Zhang, J. Lv, Self-Catalyzing chemiluminescence of luminol-diazonium ion and its application for catalyst-free hydrogen peroxide detection and rat arthritis imaging, Anal. Chem., 90 (2018) 2201–2209. https://doi.org/ 10.1021/ acs.analchem. 7b04544

[31] N.M. Mallikarjuna, J. Keshavayya, Synthesis, spectroscopic characterization and pharmacological studies on novel sulfamethaxazole based azo dyes, J. King Saud. Univ. Sci., 32 (2020) 251–259. https://doi.org/10.1016/ j.jksus. 2018.04.033

[32] N.M. Mallikarjuna, J. Keshavayya, M.P. Maliyappa, R. A. Shoukat Ali, T. Venkatesh, Synthesis, characterization, thermal and biological evaluation of Cu (II), Co (II) and Ni (II) complexes of azo dye ligand containing sulfamethaxazole moiety, J. Mol. Struc., 1165 (2018) 28–36. https:// doi.org/ 10.1016/ j.molstruc. 2018.03.094

[33] E.Q. Jasim, E.A. Alasadi, R.H. Fayadh, M.A. Muhamman-Ali, Synthesis and antibacterial evaluation of some azo-schiff base ligands and estimation the cadmium

metal by complexation, Sys. Rev. Pharm., 11 (2020) 677–687. https://doi.org/10.31838/srp.2020.6.101

[34] S. Shahab, F.H. Hajikolaee, L. Filippovich, M. Darroudi, V.A. Loiko, R. Kumar, M.Y. Borzehandani, Molecular structure and UV–Vis spectral analysis of new synthesized azo dyes for application in polarizing films, Dyes Pigm., 129 (2016) 9–17. https://doi.org/10.1016/j.dyepig.2016.02.003

[35] K. J. Al-Adilee, S. Adnan, Synthesis and spectral properties studies of novel hetrocyclic mono azo dye derived from thiazole and pyridine with some transition complexes, Orient. J. Chem., 33 (2017) 1815–1827. https://doi.org/10.13005/ojc/330426

[36] R. Alam, Synthesis and Characterization of Azo-Schiff Bases Containing Thiadiazole Moiety of Biological Interest. Thesis of Bangladesh University of Engineering and Technology, 2018. http://lib.buet.ac.bd:8080/xmlui/handle/123456789/5178

[37] G.R. Medders, F. Paesani, Infrared and Raman spectroscopy of liquid water through 'first-principles' many-body molecular dynamics, J. Chem. Theory Comput., 11 (2015) 1145–1154. https://doi.org/10.1021/ct501131j

[38] B.M. Sarhan, R.M. Rumez, H.A. Hassan, Synthesis and characterization of some new metal complexes of ethyl cyano (2-methyl carboxylate phenyl azo acetate), Ibn AL-Haitham J. Pure Appl. Sci., 26 (2013) 178–187. https://jih.uobaghdad.edu.iq/index.php/j/article/view/463/387

[39] S. D. Ahranjani, A lead analysis based on amine-functionalized bimodal mesoporous silica nanoparticles in human biological samples by ultrasound assisted-ionic liquid trap-micro solid phase extraction, J. Pharm. Biomed. Anal., 157 (2018) 1-9. https://doi.org/ 10.1016/ j.jpba.2018.05.004

[40] G.B. Vadher, R.V. Zala, Synthesis and analytical studies of some azo dyes as ligands and their metal chelates, Int. J. Chem. Sci., 9 (2011) 87–94. https://www.tsijournals.com/journals/international-journal-of-chemical-sciences.html

[41] W.J. Geary, The use of conductivity measurements in organic solvents for the characterisation of coordination compounds, Coord. Chem. Rev., 7 (1971) 81–122. https://doi.org/ 10.1016/ S0010-8545 (00)80009-0

[42] N.S. Falah, S.A.H. Abdullaha, M.S. Jabir, New azo derivative and their divalent metal ion complexes: Synthesis, characterization, and evaluation of their antibacterial activity, J. Indian Chem. Soc., 100 (2023) 101010. https://doi.org/ 10.1016/ j.jics.2023.101010

[43] T.S. Kadhim, M.M. Kareem, A.J. Atiyah, Synthesis, characterization and investigation of antibacterial activity for some new functionalized Luminol derivatives, Bull. Chem. Soc. Ethiop., 37 (2023) 159–169. https://doi.org/10.4314/BCSE.V37I1.13